ENGINEERING RESEARCH INSTITUTE
THE UNIVERSITY OF MICHIGAN
ANN ARBOR

Technical Report No. 8

AN EXPERIMENTAL STUDY OF INITIAL AND SUBSEQUENT YIELD SURFACES IN PLASTICITY

by

P. M. Naghdi
F. Essenburg
W. Koff

Project 2027

OFFICE OF ORDNANCE RESEARCH, U. S. ARMY
CONTRACT DA-20-018-ORD-12099
PROJECT NO. TB 20001(234), DA PROJECT 599-01-004

January 1957

AN EXPERIMENTAL STUDY OF INITIAL AND SUBSEQUENT YIELD SURFACES IN PLASTICITY*

By P. M. Naghdi, F. Essenburg, and W. Koff
Department of Engineering Mechanics, The University of Michigan

1. INTRODUCTION

It is well known that under a uniaxial state of stress or a state of stress due to pure torsion most materials exhibit the Bauschinger effect, i.e., possess a lower yield stress upon the reversal of the load, and for example following tension or torsion are said to be softer in compression or in reversed torsion, respectively. While under more general circumstances (such as a biaxial state of stress), no experimental evidence seems to be available with regard to the shape of subsequent yield surfaces (or loading functions) beyond the initial yield, sufficient information [see for example (1)] is available to conclude that successive yield (or loading) surfaces are not merely blown up versions of the original.

The incremental-strain theories of plasticity in general, and their stress-strain relations in particular, are dominated by the concept of a loading function, which corresponding to a given state of increments of stress predicts the absence (during unloading and neutral loading) or presence (during loading) of additional increments of plastic strains. As plastic deformation is physically an anisotropic phenomenon in character, the loading function for a work-hardening material depends on the history of loading and exhibits Bauschinger effect as well as strain-hardening anisotropy, even if the material, in the unstrained state, is isotropic. In fact as has been pointed out by Drucker (2) an isotropic work-hardening theory of plasticity cannot properly predict a Bauschinger effect during plastic deformation. It is relevant to mention here that loading functions which account for various degrees of initial and strain-hardening anisotropy as well as a Bauschinger effect have been considered by Drucker (3), Hill (4) and Edelman and Drucker (5), and that the difficulties of fitting mathematical theories of plasticity to experimental results are discussed by Stockton and Drucker (6).

*The results presented in this paper were obtained in the course of research sponsored by the Office of Ordnance Research (U. S. Army) under Contract DA-20-018-ORD-12099 with The University of Michigan.

The present paper contains experimental results for twenty-seven tubular specimens, made of a 24 S-T 4 aluminum alloy, which were initially (reasonably) isotropic. Twenty-five specimens, subjected to combined torsion-tension-reversed torsion with variable loading paths, were employed in a study of initial and two subsequent yield surfaces covering the first and the fourth quadrant of the axial stress—shear stress plane. The remaining specimens were subjected to tension alone followed by torsion (with various amounts of tension), and as in (7) enabled the determination of the initial shear modulus G_i at the initiation of twist. Although the latter type of experiment was performed on six specimens, the results for only two are reported here, since the character of the test data (except for loading paths) are the same as those described.

For the sake of clarity and for future reference it is well to call attention here to the fact that, while the specimens employed in previous investigations (7,8) were also made of a 24 S-T 4 aluminum alloy and were cut from a rolled thick plate stock possessing a rather severe initial anisotropy, the specimens employed in the present study were made of a round extruded stock, which at least by comparison (see Fig. 3) is reasonably isotropic.

2. SPECIMENS AND EQUIPMENT

The thin-walled specimens employed were made of a round extruded 24 S-T 4 aluminum alloy stock, 1 1/2 inches in diameter (the stock has an age history of about 12 years). All specimens used had the nominal dimensions of 0.75 inch ID, 0.075 inch thickness and tolerances were held to ± 0.001 inch in both eccentricity of bore and wall thickness; a detailed drawing of a typical specimen is given in (7). Initially, the specimens were reasonably isotropic as may be seen from a photomicrograph of the cross section of a typical specimen in Fig. 3 [compare with Fig. 4 in (7)]. As pointed out previously (7), it seems desirable to repeat here that the design requirements on wall thickness of the specimens were dictated by (i) elastic and plastic buckling in torsion; (ii) dimensions of the extensometer; and (iii) the available loading range of the machine.

The testing equipment employed in the present study is that used previously (7,8) with some modifications and only these modifications will be described in detail here.

The testing machine, a combined torsion-tension-reversed torsion machine, is powered by electric motors which drive the loading ram through variable speed transmissions. In order to measure the axial force and torque to which the specimen is subjected, a load cell comprising a hollow steel circular cylinder coupled in series with the specimen has been introduced. The dimensions of the load cell are so selected that it will be subjected only to elastic deformation throughout the range of loads applied to the specimen. Two Wheatstone Bridges, each consisting of eight SR-4 Type A-7 strain gages, are mounted on the surface of the cell.

The tension measuring bridge consists of gages aligned axially and circumferentially and the torque bridge consists of gages aligned at 45° to the axis of the cell. Pairs of gages comprising the various legs of the bridges are mounted at diametrically opposite positions on the cell so as to nullify any bending effects due to possible slight excentricities which might result in the loading of the cell (the calibration of the load cell also indicated an independence of tension and torque measurements). In addition to the advantage of providing for the measurement of the load in reversed torsion, the present load cell improves the previously employed set-up by coupling the cell directly in series with the specimen; all of the tension and torque in the specimen is transmitted to the load recording means (the load cell of the present set-up) whereas previously an unknown (although small) portion of the load was taken up by friction in the bearings.

In an effort to minimize the interaction of the angle of twist and the extension measurements [see Fig. 12(c) of (7)] of the previously employed extensometer, a substantial reconstruction of the extensometer shown in Figs. 1 and 2 was undertaken. The angle of twist measuring mechanism was left intact but the means of measuring extension was substantially altered. The upper and lower plates, together with the steel bearing ring, were machined to closer tolerances, and the instrument bearings were replaced with precision roller bearings. To ensure the parallelism of the upper and lower plates and to eliminate the possibility of a slight error introduced in the original design due to the utilization of removable gage blocks, three identical gage posts were added and rigidly attached to the lower plate. The gage posts are of such a length that when the upper plate is brought into contact with them (with the aid of thumb screws), the points of contact of the mounting screws are separated by precisely the gage length of the specimen (2.6250 inches). The four flexure arms were replaced by three straight flexure elements, each clamped to a support linkage. The support linkages provide each flexure element with a fixed end support and accommodate the radial displacement of the built-in end as extension takes place. As may be noted in Figs. 1 and 2, in re-designing the extensometer it was convenient to attach the bearing ring through the flexure elements and the support linkages to the top plate, and to mount the new precision roller bearings on the bottom plate; this is a reversal of the arrangement used previously [see Figs. 1 and 2 of (7)].

The recording equipment used in the present work is a Heiland Model 82-6 Bridge Balance Unit, and a Heiland 712-B oscillograph employing Heiland galvanometers (No. 40-1000) having a sensitivity of 3.1 micro-amps/inch. The sensitivities and resolutions of the four quantities measured are:

	Sensitivity	Resolution
Axial strain:	800 micro-inches/inch	± 4 micro-inches/inch
Shearing strain:	830 micro-inches/inch	± 4 micro-inches/inch
Axial stress:	4600 psi/inch	± 23 psi
Shearing stress:	4200 psi/inch	± 21 psi

It should also be mentioned that, in view of the manner in which the test was conducted, it was highly beneficial to be able to monitor the path of loading. For this purpose two independent bridges mounted on the load cell were used to activate a Mosely Autograph (X-Y plotter). The resolutions and sensitivities of the torque and tensile force measurements made by the monitoring agency were approximately one-half of those recorded by the oscillograph.

3. EXPERIMENTAL RESULTS

Twenty-five specimens were employed in order to establish sixty-eight points on the initial, a first, and a second subsequent yield surfaces in the first and fourth quadrants of the axial stress (σ_z)—shear stress ($\tau_{\theta z}$) plane. In many cases, with appropriate loading paths in combined torsion-tension-reversed torsion, a single specimen was utilized to obtain a single point on each of the three yield surfaces. The main steps in the history of a typical specimen, loaded in the first quadrant, will be described in detail as follows:

(1) The specimen, in the virgin state, is subjected to the loading path shown in Fig. 4(a). In the course of this loading the specimen is initially subjected to tension alone, followed by a torsion with tension held esentially constant, all well within the elastic range. In approaching the region where the yield surface was anticipated to lie, the path of loading consists of a combination of both tension and torsion, thus enabling the crossing of the yield surface with a straight line loading path which is oblique to the yield surface. The corresponding axial stress—axial strain and shear stress—shear strain curves are shown in Fig. 4(b,c). The time at which the inception of plastic strain is observed to occur, in Fig. 4(b,c)—the 114th second of the test, is also significantly marked on the plot of the path of loading (a reproduction of this plot is observed also by the operator during the running of the test on the X-Y plotter). Recalling that the testing machine is essentially a straining machine, it follows that for any given setting of the controls of the machine the loading path will be a straight line (not necessarily a radial path) so long as the deformation of the specimen is elastic. Since the load cell provides the specimen with an elastic support, at the inception of plastic strains (with the deformation rates held constant), an appreciable deviation from the straight line loading path will be observed. Thus, in summary, two methods of observing the inception of yield are available: The first, and most reliable, is the observation of the time of the inception of plastic strains on the stress-strain plots of Fig. 4(b,c), which is an a posteriori method since they are obtained from the developed oscillograph film. Incidentally, this criterion for observing the inception of yield is similar to that employed by Taylor and Quinney (9). The second method, which gives the same results as the first although less reliably, is the observation of a change in the direction of the loading path (with the deformation rates held constant) on both the oscillograph record and the monitoring agency. While, in order to obtain a point on the initial yield surface

it was necessary to slightly "pierce" this surface, it should be noted that, the magnitude of the increments of plastic strain involved in this "piercing" are small compared with the plastic strains in the next step of the procedure.

(2) As soon as the yield surface is reached the specimen is unloaded (elastically) to the state of zero stress, and next loaded in torsion alone to reference point A indicated in Fig. 4(a). As will be seen presently this reference point plays a dominant role in establishing the first subsequent yield surface. After unloading, from reference point A, the specimen is then subjected to the loading path shown in Fig. 4(d) with corresponding axial stress—axial strain and shear stress—shear strain curves shown in Fig. 4(e,f), and the inception of the first subsequent yield surface is recognized in a manner similar to that used in the recognition of the initial yield surface.

(3) The specimen is again unloaded to the state of zero stress and loaded in torsion to reference point B, which establishes the second subsequent yield surface. After unloading, the specimen is then subjected to the loading path shown in Fig. 4(g) with corresponding axial stress—axial strain and shear stress—shear strain curves shown in Fig. 4(h,i). The reaching of the second subsequent yield surface is again recognized by the technique described above.

The main steps in the history of another typical specimen, loaded in the fourth quadrant of the σ_z - $\tau_{\theta z}$ plane, including the loadings to reference points A and B, are similar to those described above. The plots for such a typical specimen, similar to those of Fig. 4, are shown in Fig. 5, where for convenience of presentation the images of references points A and B are also indicated. It should be emphasized, however, that the reference points A and B lie on the positive $\tau_{\theta z}$-axis and that all specimens are referred to these points irrespective of their loading paths. The experimentally determined initial and subsequent yield surfaces are shown in Fig. 6.

The role played by reference points A and B, in establishing the first and second subsequent yield surfaces, requires further elaboration: Prior to the use of any given specimen to determine a point on the first subsequent yield surface, it is first loaded to reference point A, and this loading is accompanied by a substantial amount of plastic deformation which is large in comparison with that resulting from the slight "piercing" of the initial yield surface mentioned above. Thus, prior to the time at which the specimens are used to determine points on the first subsequent yield surface, all (except for possible slight differences in the "piercing" of initial yield) have had identical strain-hardening histories. In a similar manner, the loading of all specimens to reference point B establishes the second subsequent yield surface.

As noted earlier, in addition to the results shown in Fig. 6, six virgin specimens were subjected to tension well into the plastic range, followed by torsion with varying amounts of tension, primarily to determine the initial shear modulus G_i at the beginning of twist. The plots of experimental results for two typical specimens, arranged similar to those reported in (5), are shown in Figs. 7 and 8.

4. DISCUSSION OF RESULTS

With reference to Fig. 6, it is observed that: (1) the initial yield surface is essentially symmetric about the σ_z-axis; (2) the first and second subsequent yield surfaces, in the neighborhood of the $\tau_{\theta z}$-axis, display a pronounced Bauschinger effect which gradually vanishes as the curves approach the σ_z-axis; and (3) the initial yield surface, except for a slight deviation in the vicinity of the σ_z-axis, is almost identical with the Mises yield condition.

Although the initial yield surface may be well fitted by an isotropic stress theory of plasticity (where the loading function is dependent on the stress invariants only), to fit the initial and subsequent yield surfaces of the present study, the loading function of an anisotropic strain-hardening theory must be employed. Such a comparison with the mathematical theory of plasticity, though desirable, constitutes a formidable task and will not be attempted here.

As seen in Figs. 7 and 8, comparison of the elastic shear modulus (G_o) and the initial shear modulus at the initiation twist (G_i), reveal that they are essentially equal. In all cases (including the results of the four specimens not reported here), the percentage deviation between G_o and G_i is about 5 per cent or less. This result (i.e., $G_i = G_o$ during both loading and unloading) which is in agreement with that reported in (10), support the prediction of all isotropic incremental-strain theories of plasticity involving a plastic potential. The difference in the values of G_i of the present paper and those given previously should be attributed to the character of the material employed in (7) which, as noted earlier possessed a rather severe initial anisotropy.

REFERENCES

1. "Über den Zusammenhan von Spanungen und Formäenderungen in Verfestigungsgebeit", by R. Schmidt, Ingenieur Archiv, 3, 215-235 (1932).

2. "Relations of Experiment to Mathematical Theories of Plasticity", by D. C. Drucker, J. Appl. Mech., 16, 349-357 (1949).

3. "The Significance of the Criterion for Additional Plastic Deformation of Metals", by D. C. Drucker, J. Colloid Science, 4, 299-311 (1949).

4. "Mathematical Theory of Plasticity", by R. Hill, Clarendon Press, 1950.

5. "Some Extensions of Elementary Plasticity Theory", by F. Edelman and D. C. Drucker, J. Franklin Inst., 251, 581-605 (1951).

6. "Fitting Mathematical Theories of Plasticity to Experimental Results", by F. D. Stokton and D. C. Drucker, J. Colloid Science, 5, 239-250 (1950).

7. "An Experimental Study of Biaxial Stress-Strain Relations in Plasticity", by P. M. Naghdi and J. C. Rowley, J. Mech. Phys. Solids, 3, 63-80 (1954).

8. "Experiments Concerning the Yield Surface and the Assumption of Linearity in the Plastic Stress-Strain Relations", by P. M. Naghdi, J. C. Rowley, and C. W. Beadle, J. Appl. Mech., 22, 416-420 (1955).

9. "The Plastic Distortion of Metals", by G. I. Taylor and H. Quinney, Trans. Roy. Soc. (London), A230, 323-362 (1931).

10. "Experimental Studies of Polyaxial Stress-Strain Laws of Plasticity", by B. Budiansky, N. F. Dow, R. W. Peters, and R. P. Shepherd, Proc. First U. S. Natl. Cong. Appl. Mech., 503-512 (1951).

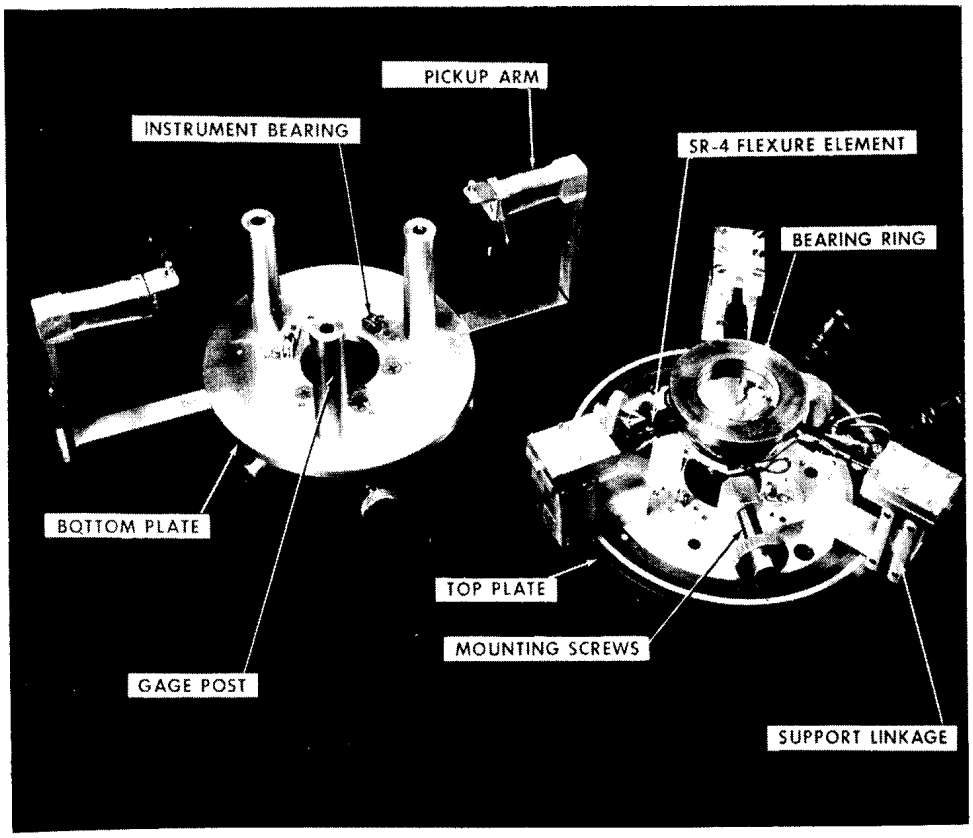
PICKUP ARM
INSTRUMENT BEARING
SR-4 FLEXURE ELEMENT
BEARING RING
BOTTOM PLATE
TOP PLATE
MOUNTING SCREWS
GAGE POST
SUPPORT LINKAGE

Fig. 1

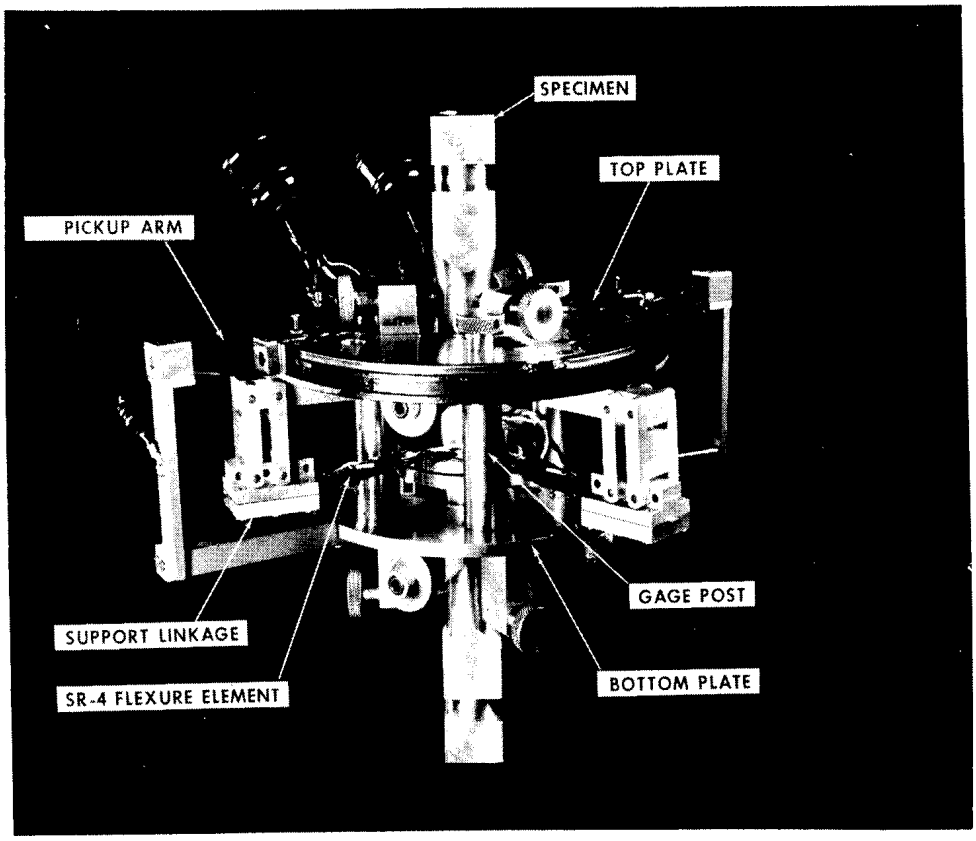
SPECIMEN
TOP PLATE
PICKUP ARM
GAGE POST
SUPPORT LINKAGE
SR-4 FLEXURE ELEMENT
BOTTOM PLATE

Fig. 2

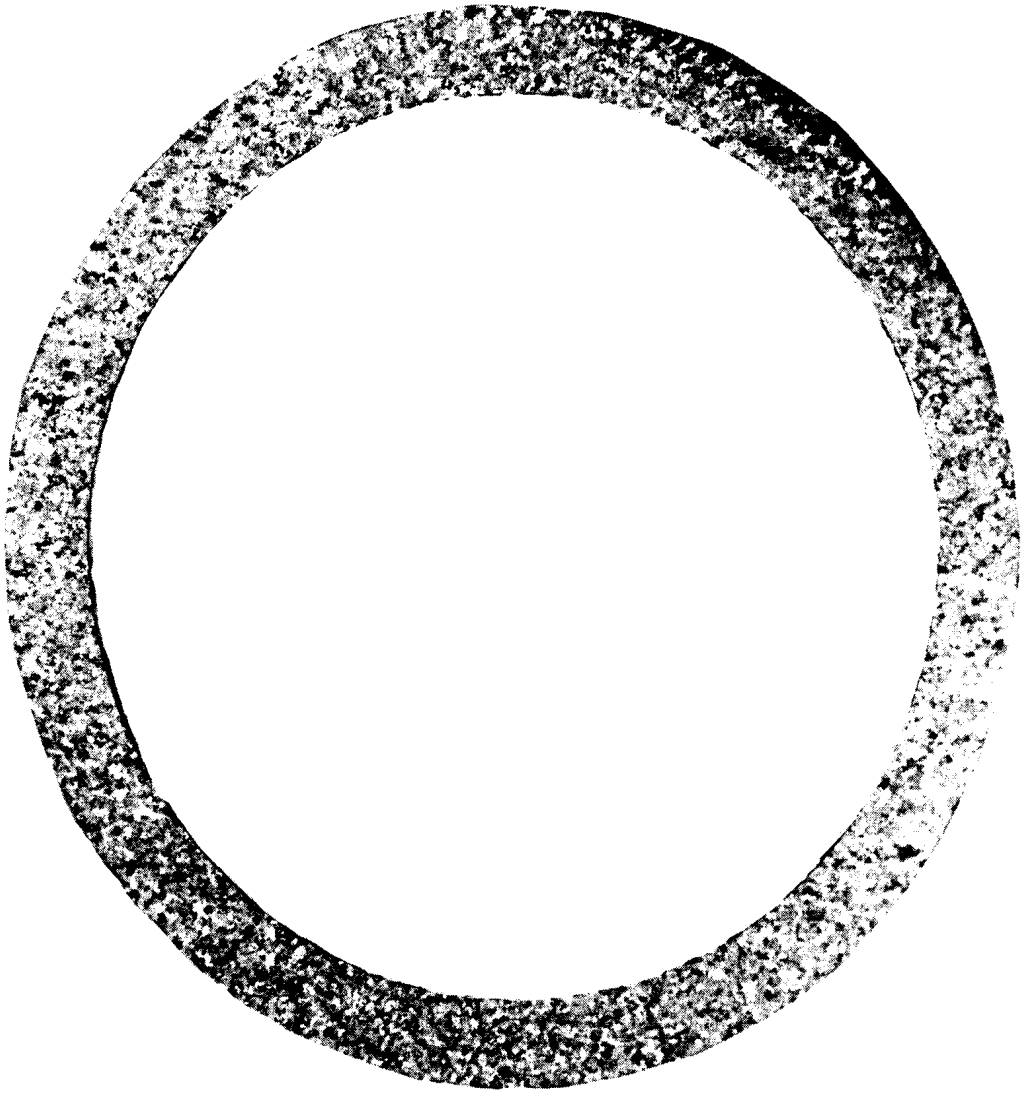

Fig. 3

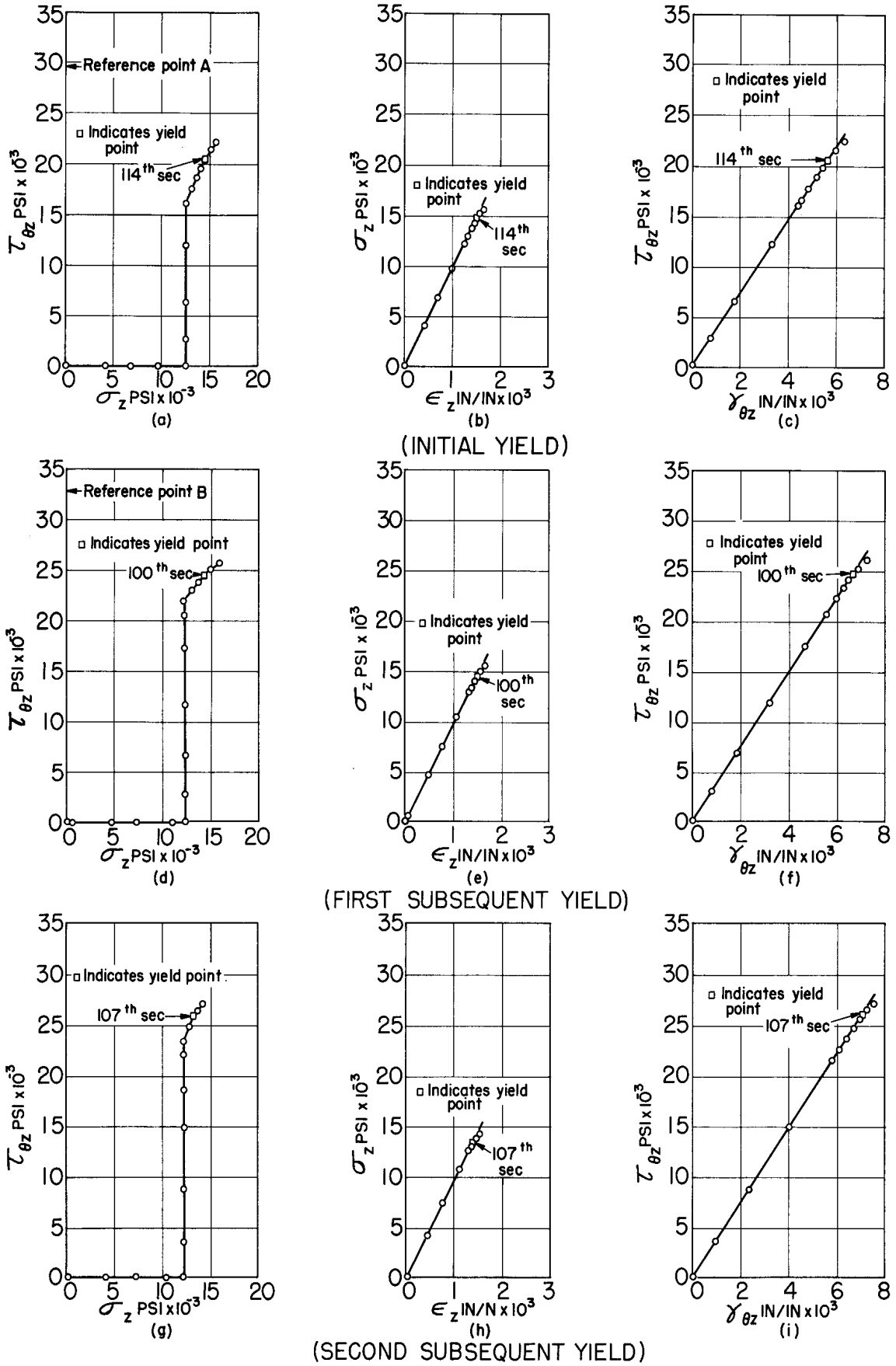

Fig. 4. Loading path and stress-strain curves for the determination of the initial and subsequent yield points of a typical specimen (No. 89) in the first quadrant.

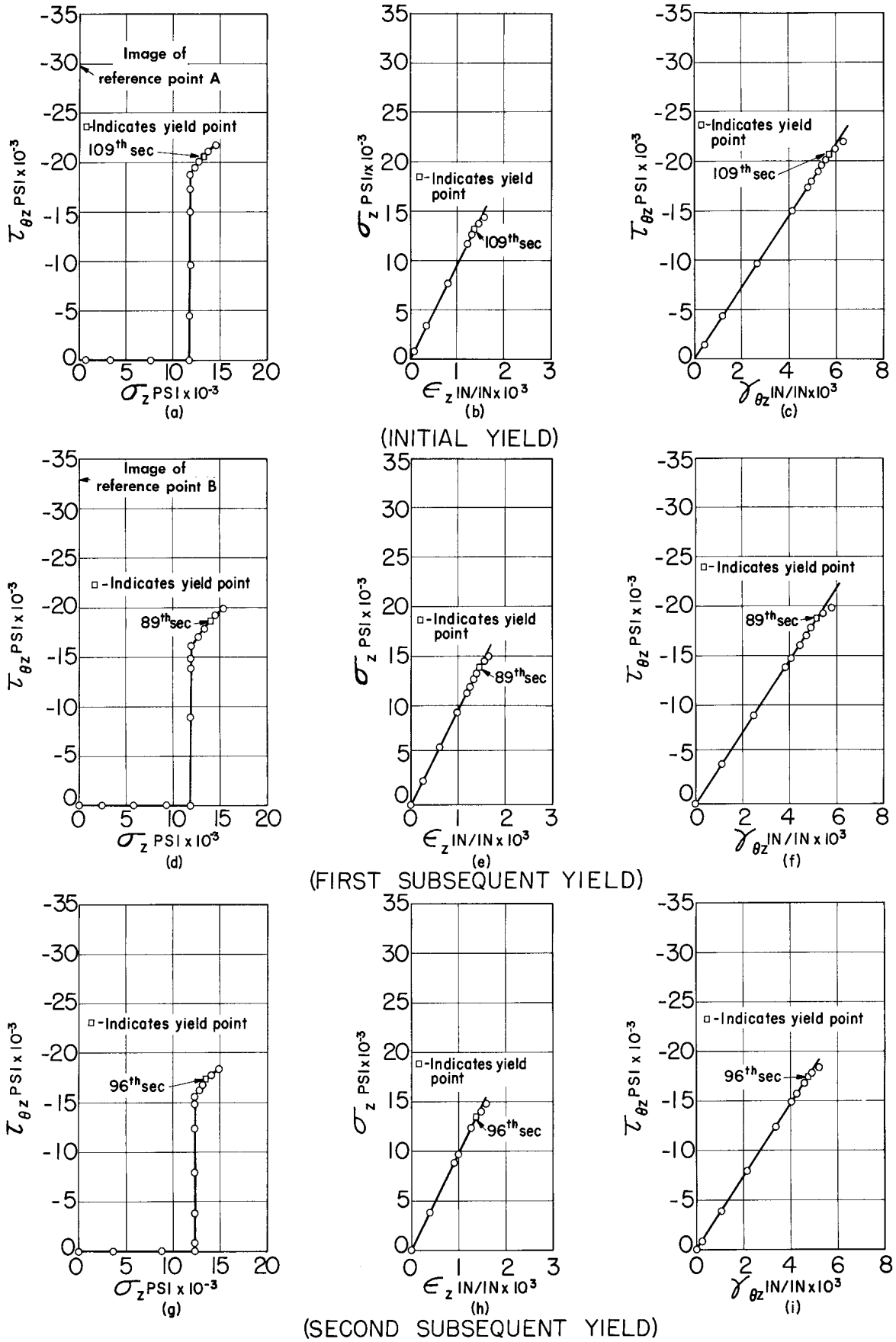

Fig. 5. Loading path and stress-strain curves for the determination of the initial and subsequent yield points of a typical specimen (No. 91) in the fourth quadrant.

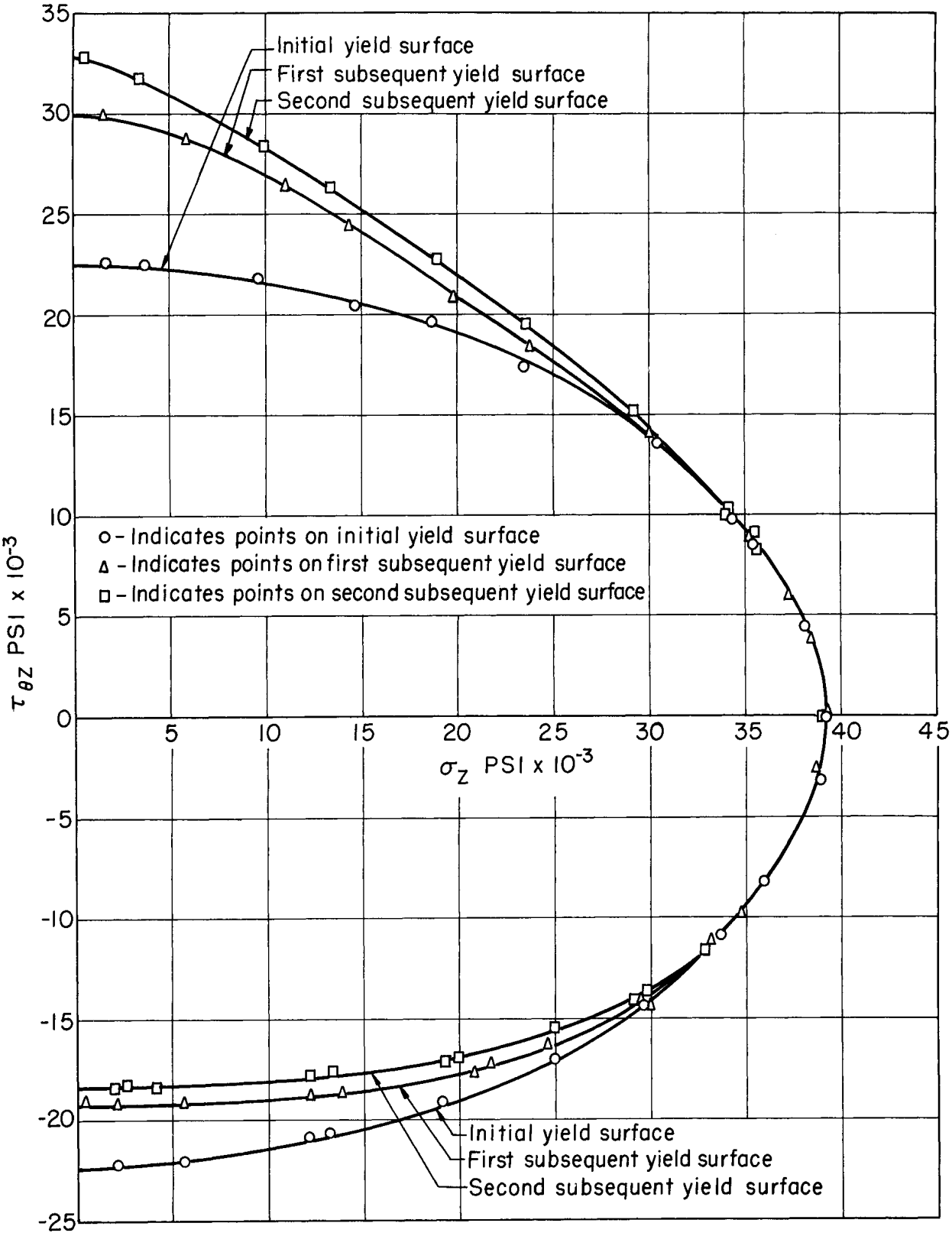

Fig. 6. The initial and subsequent yield surfaces.

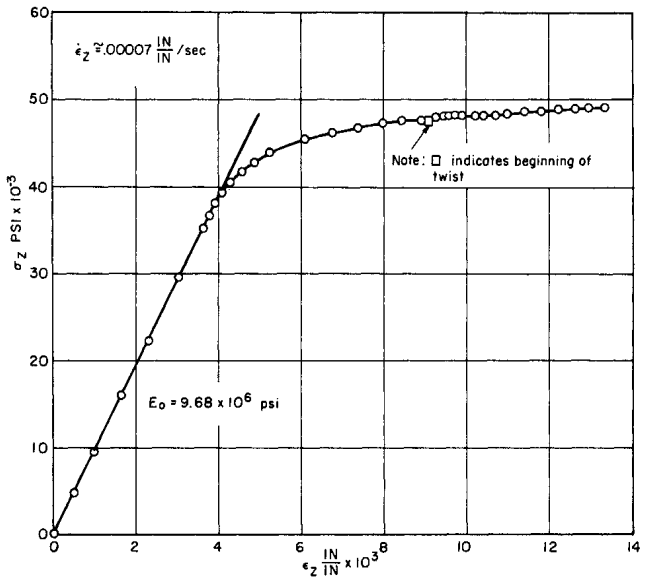

Fig. 7(a). Axial stress vs axial strain (Specimen No. 114).

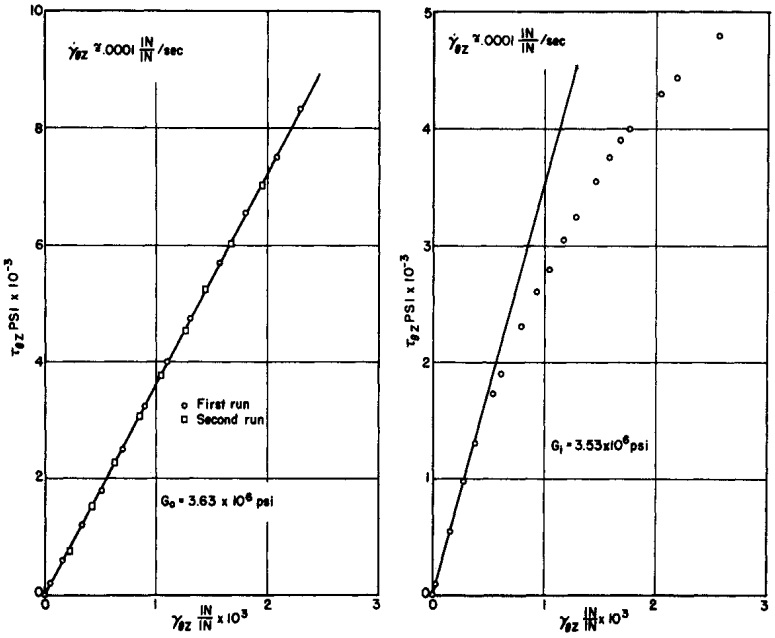

Fig. 7(b). Elastic and initial shear moduli (Specimen No. 114).

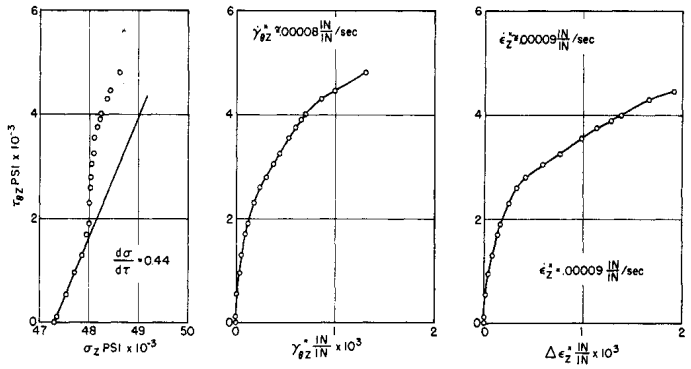

Fig. 7(c). Plastic strains and loading path (Specimen No. 114).

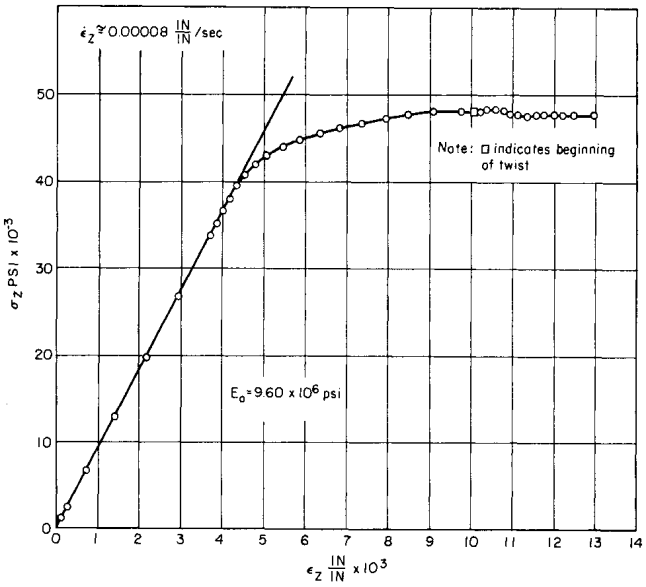

Fig. 8(a). Axial stress vs axial strain (Specimen No. 115).

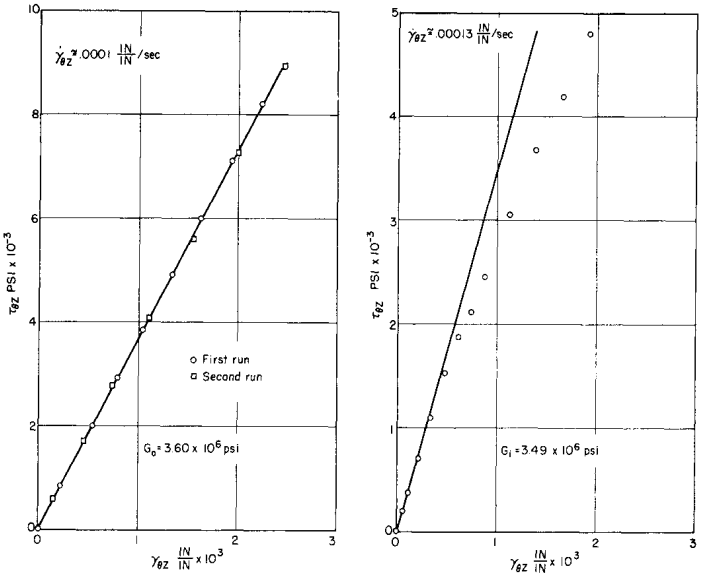

Fig. 8(b). Elastic and initial shear moduli (Specimen No. 115).

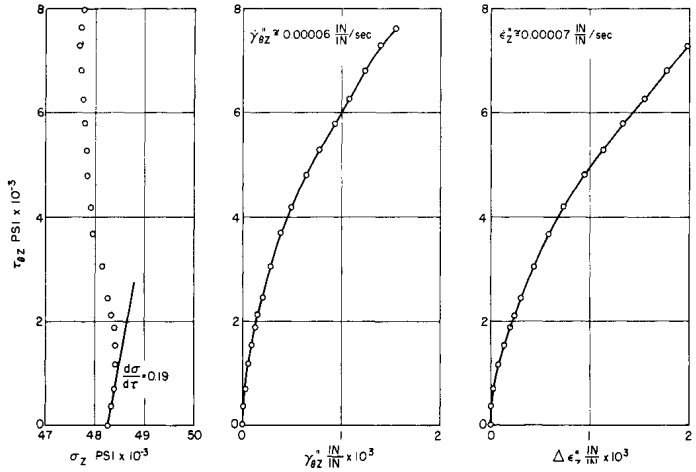

Fig. 8(c). Plastic strains and loading path (Specimen No. 115).